MILITARY TECHNICAL COLLEGE
CAIRO - EGYPT

Two Adaptive Algorithms for Target Detection in Cluttered Images

A.S. El-Fishawy* and S.B.Kesler**

ABSTRACT

Detection of targets in in a low signal to clutter plus noise ratio (SCNR) is a problem of increasing interest. In this paper we present two adaptive algorithms for the detection of small targets (of the order of one pixel) in images using reference correlated frames (the reference frames can be obtained either from frequency bands of the same scene or from different sequential observation in time) in a low signal to clutter plus noise ratio (SCNR) environment (of the order of -14.5 dB). They both have the ability to track the nonstationary image signals (targets and clutter plus noise) and suppress the clutter plus noise background. Both detectors are based on time varying autoregressive models to model image background and on correlation canceling concept. The first one uses an order recursive least squares (ORLS) lattice filter, while the second one is based on a normalized version of the two dimensional least mean square (TDLMS) algorithm. The influence of the order of the detectors on their detection performance is studied. The performance of the two algorithms are evaluated using an optical satellite image, as a clutter background, with computer generated target and noise added to it.

* Assistant Professor, Dpt. of Communications Eng., Menoufia Unifersity, Menouf, Menoufia, Egypt.
** Associate Professor, Dpt. of Electrical and Computer Eng., Drexel University, Phila, Pa 19104, USA

I. INTRODUCTION

Detection of unfriendly targets is an integral part of the air, ground and sea defense. The area under surveillance is monitored by a set of receivers, active and/or passive. The receivers (sensors) are intercepting the energy which is reflected from, and/or radiated by targets of interest. The received signal, in addition to the desired information, usually contains heavy clutter and background noise. In such environment, target detection procedures should be able to isolate the moving target in signal-to-clutter-plus-noise ratios (SCNR) in the order of -10 to -20 dB. Clutter sources themselves are not entirely spatially stationary, even during the relatively short time spans. Weather clutter is slowly moving due to wind activities, and clear air turbulence, among other causes. Even ground clutter is varying with the local movement of vegetation. Sea clutter exhibits various statistical characteristics in different sea states.

Gagliari et. al [1] have developed an algorithm for the detection of optical targets by using correlated reference scene. However, this algorithm demands a substantial computation time, most of which is used for estimating the covariance matrix and for calculating matrix inverses. Margalit et. al [2] have developed a detection algorithm which is based on the assumption that the image intensity is spatially Gaussian process and that the covariance matrix of optical and infrared (IR) images, after subtraction of correct variable mean, is approximately a constant times an identity matrix. Therefore, the resulting Gaussian image processes are nearly white. This algorithm was shown to save most of the computation time required by the optimum algorithm developed in [1]. In addition, Chen and Reed [3] have developed an alternate algorithm for the detection of optical target by using a reference scene. The above algorithms are based on the approximation of the image data by a white Gaussian process. For real images, this assumption is not necessarily valid in general case.

To remedy the mentioned problems, we suggest two adaptive algorithms for clutter plus noise suppression and optical/infrared targets detection. The first one is based on the order recursive least-squares (ORLS) lattice algorithm [4,5], while the second processor uses a normalized version of the two dimensional least mean square algorithm (TDLMS) [5,6].

PROBLEM FORMULATION

Let us assume that we have two M by N images of a specific scene that are taken at different times. These images can be forward looking infrared (FLIR), radar echo, remote sensing. The first (primary) image, $d(m', n')$, differs from the second (reference) one, $x(m', n')$, in that it has a target embedded in a background clutter. The m' ($=0,1,\ldots,M-1$) and n' ($= 0,1,\ldots,N-1$) are the spatial coordinates of the pixel location with respect to some prespecified coordinate system, say, with the origin in the upper left corner. The background in the reference image may be shifted or blurred and may be of different brightness compared to the background in the primary one. The backgrounds, however, remain spatially correlated, while independent of target component.

Our objective is to design adaptive target detector that should have the ability to track the nonstationary image signals, suppress the background and efficiently detect the changes (targets) between two images in a sequence in a low signal to clutter plus noise ratio (of the order of -14.5 dB). Target image edges should be preserved so that relatively small size target can be discerned. In the applications where images appear in sequence, both adaptive algorithms can be applied to a pair consisting of a current frame and a reference one.

General block diagram of the suggested target detectors is shown in Fig.1. Signals and processor parameters are given as 1-D functions of spatial coordinates as they will be used in the context of the ORLS processor. For the origin in the upper left corner of M by N image, the value of the single spatial coordinate n is related to m' and n' as:

$$n = m'N+n';\ n'=0,\ldots,N-1,\ m'=0,\ldots,M-1$$

and n runs from 0 to MN-1. Thus, for the "zeroth" row ($m'=0$), $n=n'$($=0,\ldots,N-1$),for the first row ($m'=1$),

n' (= 0,1,...,N-1) are the spatial coordinates of the pixel location with respect to some prespecified coordinate system, say, with the origin in the upper left corner. The background in the reference image may be shifted or blurred and may be of different brightness compared to the background in the primary one. The backgrounds, however, remain spatially correlated, while independent of target component.

Our objective is to design adaptive target detector that should have the ability to track the nonstationary image signals, suppress the background and efficiently detect the changes (targets) between two images in a sequence in a low signal to clutter plus noise ratio (of the order of -14.5 dB). Target image edges should be preserved so that relatively small size target can be discerned. In the applications where images appear in sequence, both adaptive algorithms can be applied to a pair consisting of a current frame and a reference one.

General block diagram of the suggested target detectors is shown in Fig.1. Signals and processor parameters are given as 1-D functions of spatial coordinates as they will be used in the context of the ORLS processor. For the origin in the upper left corner of M by N image, the value of the single spatial coordinate n is related to m' and n' as:

$$n = m'N + n';\ n' = 0,\ldots,N-1,\ m' = 0,\ldots,M-1$$

and n runs from 0 to MN-1. Thus, for the "zeroth" row ($m'=0$), $n=n'$($=0,\ldots,N-1$),for the first row ($m'=1$), $n=N+n'$($=N,N+1,\ldots,2N-1$), and so on, until the (M-1)st row ($m'=M-1$) where $n=(M-1)N+n'$ ($=MN-N,MN-N+1,\ldots,MN-1$). The 1-D representation for the ORLS processor is adequate since it converges rapidly for even the moderate level of 1-D crosscorrelation between horizontal lines in two images. For the TDLMS algorithm, the block diagram would be the same, except that all the signals and filter parameters would be two-dimensional functions of spatial coordinates instead of one-dimensional. The primary image input d(n) (recent frame) consists of the desired target signal t(n) embedded in a clutter background s(n) and a colored noise $v_1(n)$. In terms of Wiener filtering theory, d(n) represents the desired response. The reference input x(n) consists of a clutter (possibly blurred), $s_b(n)$, and a colored noise, $v_2(n)$, which is spatially correlated with that of the primary image. The colored noises $v_1(n)$ and $v_2(n)$ can be considered as additional clutter sources.

Defining the L-th order filter coefficient vector by $\mathbf{w} = [w_0, w_1, \ldots, w_{L-1}]^T$ and the Lx1 reference input vector as $\mathbf{x}(n) = [x(n), x(n-1), \ldots, x(n-L+1)]^T$, the output of the target detector in Fig.1, at spatial coordinate n, is given by

$$y(n) = d(n) - z(n) = d(n) - \mathbf{w}^T\mathbf{x}(n)$$

where the primary input is

$$d(n) = t(n) + z(n) \quad \text{and} \quad z(n) = s(n) + v_1(n) \tag{1}$$

is the clutter plus noise component of primary input and t(n) is the target signal component embedded in the primary frame. The optimum Wiener solution, $\mathbf{w}_{opt}$, of the tap vector $\mathbf{w}$, which minimizes the mean square (MS) value of the output y(n) is given by

$$\mathbf{w}_{opt} = \Phi^{-1}_{xx}\Psi_{dx} \tag{2}$$

where Φ_{xx} is the reference input autocovariance matrix given by

$$\Phi_{xx} = E[\mathbf{x}(n)\mathbf{x}(n)^T]$$

and Ψ_{dx} is the cross-covariance vector between the input vector x(n) and the desired signal d(n) as:

$$\Psi_{dx} = E[d(n)\mathbf{x}(n)]. \tag{3}$$

The "minimum" output of the change detector, that is, the output having minimized energy, which corresponds to the optimum filter is

autocovariance matrix, $\Phi(n)$, of the reference input vector, $\mathbf{x}(n) = [x(n),x(n-1),\ldots,x(n-l+1)]^T$, and the Lx1 cross-covariance vector, $\Psi(n)$, between $\mathbf{x}(n)$ and the desired input, d(n), as follows [8]:

$$\Phi(n) = \Phi(n-1) + \sum_{i=0}^{L-1}\sum_{j=0}^{L-1} \mathbf{x}(n-i)\mathbf{x}(n-j)$$

$$\Psi(n) = \Psi(n-1) + \sum_{j=0}^{L-1} d(n)\mathbf{x}(n-j)$$

After $\Phi(n)$ and $\Psi(n)$ are updated for a given n, the reflection coefficients $K^f_m(n)$, $K^b_m(n)$ and $H_m(n)$ are order-updated using $E_{m-1,0,0}(n)$, $R_{m-1,0,0}(n)$, $C_{m-1,0,0}(n)$ and $D_{m-1,0,0}(n)$, and the GRE's of order m are obtained by using the values at m-1, and the reflection coefficients of order m. Once the adaptation is performed, the signal $y_{min}(n)$ represents the difference image, i.e., $y_{min}(n) = g_{L-1}(n) = t(n)$, which contains the target to be detected.

The TDLMS Target Detector:

The 2-D counterpart of the Widrow LMS algorithm was originally introduced by Hadhoud and Thomas [6] for handling 2-D signals. It is well suited for our problem because of the assumption of image background correlatedness in both dimensions. The TDLMS algorithm employs the method of the steepest decent, and the current filter weight matrix is given by the previous weight matrix plus a change proportional to the negative gradient of the error power. Referring to Fig.4, the 2-D arrays $\mathbf{x}$ and $\mathbf{d}$ are the reference and primary inputs, respectively, both of dimension M by N. The filter weight matrix is of dimension K by L. In the example in Fig.4, M=5, N=10, K=2 and L=5. Of course, the 2-D algorithm reduces to its 1-D counterpart for K=1. When the filter is operating on the neighborhood of the pixel x(m,n), as indicated in Fig.4, the error signal at the j-th iteration, $y_j(m,n)$ is given by

$$y_j(m,n) = d(m,n) - z_j(m,n) = d(m,n) - \sum_{k=0}^{K'-1}\sum_{l=0}^{L'-1} w_j(k,l)x(m-k,n-l)$$

In the above equation mruns from 0 to M-1 and n runs from 0 to N-1. Limits K' and L' are equal, respectively, to K and L for $m \geq K-1$ and $n \geq L-1$. Towards the image boundaries, where $m < K-1$ and/or $n < L-1$, K' and L' reduce, respectively to m and n. When the filter window scans the image left-to-right, and top-to-bottom iteration index is related to the current pixel coordinates by

$$j = mN + n \qquad n = 0,\ldots,N-1 \text{ and } m=0,\ldots,M-1$$

The weight adjustment algorithm is then given by

$$\mathbf{w}_{j+1}(k,l) = \mathbf{w}_j(k,l) + 2\mu\, y_j(m',n')x(m'-k,n'-l),$$

The value of μ is chosen to balance the tradeoff between the convergence speed, tracking ability and steady-state MSE. To optimize the convergence factor μ, different ways were sugessted for 1-D gradient-based adaptive algorithms. We use a normalized value of μ [9,10], i.e.,

1. The sugessted target detector could suppress the clutter and noise background components while keeping the target power unattenuated.

2. The Wiener solution requires prior information about the covariance matrix of the clutter plus noise. However, in most practical situations, that required statistics is seldom known in advance, and typically, it varies with time. Therefore, the most effective solution for target detection relies on the use of adaptive filters.

III. ADAPTIVE ALGORITHMS FOR TARGET DETECTION

Assume available a recent frame, d(n), which contains a target embedded in a clutter plus noise background. Adaptive target detectors can be developed by using information that the clutter signals in the recent frame and in a reference frame are spatially correlated.

The error signal y(n), y(m,n) in the case of TDLMS algorithm, is used to generate the performance criterion for adjusting the filter coefficients. The adaptive filter (ORLS lattice or TDLMS) uses the reference input frame to estimate the clutter plus noise background in the primary Input frame. Then, the estimated clutter plus noise is subtracted from the primary input, leaving only the estimate of the target which we wish to detect.

The performance criterion for the TDLMS is to minimize the least mean square of value $y(m', n')$, as the name implies. On the other hand, the exact least squares (ELS) algorithms perform the minimization of the finite sum of L values of $y(n)^2$ which is known exactly for each step n. Here, we treat the variant of ELS, known as the order-recursive least squares (ORLS) lattice algorithm.

The Adaptive ORLS Algorithm

Fig.2 shows the joint lattice filter of order L, where $e_m(n)$ and $r_m(n)$ are, respectively, the forward and backward residual at spatial location n, of the inverse filter part of the lattice, corresponding time-varing reflection coefficients are $K^f_m(n)$ and $K^b_m(n)$. The joint path input $g_0(n)$ is the primary image d(n), whereas the reference image x(n) is fed to the inverse filter input. The backward residuals $r_m(n)$ are weighted by joint reflection coefficients $H_m(n)$ to obtain the estimates, z(n), of the clutter plus noise component, z(n), of the primary image d(n), and these are then subtracted from $g_m(n)$ to yield the estimate, $\hat{y}(n)$, of the desired target, $\hat{y}(n) = g_{L-1}(n)$.

We use the ORLS lattice algorithm for computing the reflection and joint coefficients of the lattice filter. This algorithm differs from the conventional LS lattice [7] in that the time and order recursions are separated as shown in Fig.3. The problem of poor initial speed of convergence of the mixed time and order recursive LS lattice algorithms and the related gradient lattice algorithms in a fixed-point environment have been alleviated. Since this approach does not require residual recursions, error accumulation does not occur, and hence there is no degradation of the adaptation speed.

The generalized residual energies (GREs) are LxL matrices derived from the autocovariances of $e_m(n)$, $r_m(n)$, $g_m(n)$, and the cross-covariances between them, and are defined as follows [4,5]:

$$E_{m,i,j}(n) = e^T_m(n-i)\, e_m(n-j),$$
$$R_{m,i,j}(n) = r^T_m(n-i-1)\, r_m(n-j-1),$$
$$C_{m,i,j}(n) = e^T_m(n-i-1)\, r_m(n-j-1),$$
$$D_{m,i,j}(n) = g^T_m(n-i)\, r_m(n-j-1),$$
$$A_{m,i,j}(n) = g^T_m(n-i)\, e_m(n-j).$$

where $0 \le i,j \le L-1$. At each pixel location n, "the covariance matrix tracking" block of Fig.3 updates the LxL

$$\mu_j = \frac{\mu_0}{(LK)(\sigma_j^2)} \quad , \quad 0 < \mu_0 < 1$$

where LK is the number of filter coefficients and σ^2_j is the power estimate of the reference frame which is updated for the current input pixel value x(m,n) as follows

$$\sigma_j^2 = \alpha\, x^2(m,n) + (1 - \alpha)\, \sigma_{j-1}^2 \quad , \quad 0 \le \alpha << 1$$

and α is a forgetting factor. This estimate fits nonstationary environment assumption since α can be selected to reduce the influence of past input pixels. The initial value of σ^2_j is the *a priori* estimate of the input power of the reference frame x(m,n). In many application, images are often of the square shape, i.e., M=N. Also the window size is taken to be square, resulting in K=L.

IV COMPUTER SIMULATION RESULTS

In an experimental verification of the two adaptive target detectors, an optical satellite image s(n) of a city area, of size 42x42 as shown in Fig.5, is used as a clutter background for both the primary input, d(n), and the reference input, x(n). The primary input is formed from s(n) by adding to it a colored noise, $v_1(n) = a_1 v_1(n-1) + v(n)$ where v(n) is zero mean white Gaussian noise of variance σ and a one pixel target centered at spatial location m=14, n=24 . Therefore,

$$d(n) = t(n) + z(n), \text{ where } \quad z(n) = s(n) + v_1(n)$$

Such a composite primary image input is shown in Fig.7. The reference image input, x(n), is a blurred version of s(n) with a colored noise $v_2(n)$ (correlated with $v_1(n)$) as shown in Fig.8. Blurring is performed by passing s(n) through a low-pass filter, e.g,

$$s_b(n) = 0.95\, s_b(n-1) + 0.05 s(n)$$

Therefore,

$$x(n) = s_b(n) + v_2(n)$$

where $v_2(n) = a_2\, v_2(n-1) + v(n)$ and v(n) is white gaussian noise. It can be shown that the crosscorellation between $v_1(n)$ and $v_2(n)$, $\psi_{v1v2}(k)$, is

$$\psi_{v_1 v_2}(k) = \frac{a_1^k}{1 - a_1 a_2}\, \sigma_n^2 \quad , \qquad k \ge 0 \qquad (6)$$

and the correlation coefficient, $r_{v1v2}(k)$, will be

$$r_{v_1 v_2}(k) = \frac{\psi_{v_1 v_2}(k)}{\sqrt{\sigma_{v_1}^2\, \sigma_{v_2}^2}}\, \sigma_n^2 \qquad (7)$$

Sustituting with equation (6) in equation (7), the correlation coefficient for zero lag, $r_{v_1v_2}(0)$, will be

$$r_{v_1v_2}(0) = \frac{\sqrt{(1-a_1^2)(1-a_2^2)}}{(1-a_1a_2)} \leq 1$$

We choose $a_1 = -0.5$ and $a_2 = 0.8$ such that $\psi_{v_1v_2}(0)$ and $r_{v_1v_2}(0)$ will be equal to 0.7142 and 0.3712, respectively. To quantify the SCNR in the input and output images, the power of the clutter plus noise in the primary input z(n) is computed as:

$$P_z = (1/MN) \sum_{i=0}^{MN-1} (s^2(i) + v^2_1(i)),$$

where the pixel location is taken to be in one dimension and the images are of size M by N. Similarly, the power of the target image signal is computed:

$$P_t = (1/Q^2) \sum_{i=0}^{Q^2-1} t^2(i),$$

where Q is empirically selected size of the square window that encompases the target.
Thus, the input $SCNR_i$ is given by

$$SCNR_i = P_t/P_z,$$

The output of the target detector $y_{min}(n)$ consists of the estimated target signal in addition to the residual clutter plus noise. The output SCNRo is

$$SCNR_o = [(1/Q^2) \sum_{i=0}^{Q^2-1} ch^2(i)) / ((1/MN) \sum_{i=0}^{MN-1} (y(i) - ch(i))^2]$$

The two adaptive detection algorithms are applied to the primary and reference images of Figs.6 and 7, respectively. For convenience, the $SCNR_i$ of the primary image d(n) was chosen to be -14.5. The powers of the colored noises $v_1(n)$ and $v_2(n)$ were adjusted so that the clutter to noise ratio (CNR) in the primary input is equal to 24.4 dB. For the ORLS processing, images are processed row by row sequentially so as to represent the one-dimensional input to a filter of order L=2. The output, $\hat{t}(n)$, of the ORLS detector is shown in Fig.8. The choice of L=2 for the order of the lattice was guided by its effect on the improvement factor, which is shown in Fig.9. The optimal value for L is 4, however, the difference in performance for any value of L greater than one all the way up to L=10 is negligibly small. The choice of minimum value in this range speeds up the computation significandy. The $SCNR_o$ and the improvement factor were 28.63 dB and 43.13 dB, respectively.

The TDLMS detector with a window size of 2x2 pixels, a convergence factor μ_0=0.047, a forgetting factor α=0.01, and an initial power estimate of x(m,n) of 0.02 was used to scan the images left-to-right, and top-to-bottom. The resulting output is shown in Fig.10. Again the target is clearly visible, indicating the powerful detection capabilities of the proptsed detectors. Compared to the output of the ORLS in Fig.4.9, however, the detected target is of a lower intensity due to a generally slower convergence of the TDLMS. The first row of the output image shows strong clutter background due to the same effect, combined with the fact that the window 'size' is reduced to 2x1 pixels. The $SCNR_o$ and improvement factor values of 8.1 dB and

22.58 dB, respectively.

V. CONCLUSIONS:

The presented results show that both the suggested adaptive target detectors display good performance for the detection of small size target (of the order of one pixel) embedded in cluttered images.

Neither target detectors requires any prior information about the shape or position or the statistics of the change, or the statistics of clutter and noise, except that the background clutter and noise in the primary and reference images are spatially correlated. Also, the target image/target and the clutter plus noise backgrounds are assumed to be uncorrelated. The background in the reference image can be scaled and/or blurred and/or have different brightness from the primary one. Both the suggested change detectors could successfully track the nonstationary image signals, suppress the clutter and noise background and detect the change between the images in a very low signal to clutter and noise environments (SCNR of the order of -14.5 dB).

The order recursive least squares (ORLS) target detector; however, is more robust in very low signal to clutter ratio environments. It converges very quickly, within about 2L iterations, and does not require adjustment of any tuning parameters. It is relatively insensitive to finite word length effects, and can easily be implemented by using systolic architecture, so that the computation time can be drastically reduced.

The TDLMS target detector is computationally as efficient as its 1-D counterpart, requires the order of 2(LxK) multiplication per iteration. Its convergence is, however, slow which may result in insufficient background suppression in the upper-left region of the image. It needs adjustments of the convergence factor and about 300 to 400 iterations for the algorithm to converge.

REFERENCES

[1] R. M. Gagliardi, I. S. Reed, H. M. Shao, and A. Margalit, "Optical Target Detection Using Dual Scene Observation," Univ. of Southern California, Electrical Engineering, Report, Feb. 1983.

[2] A. Margalit, I. S. Reed, and R. M. Gagliardi, "Adaptive Optical Target Detection Using Correlated Images," IEEE Trans. Aerospace and Electronic Systems, vol. AES-21, no .3 , May 1985, pp 494-405.

[3] J. Y. Chen and I. S. Reed, "A Detection Algorithm for Optical Targets in Clutter," IEEE Trans. Aerospace and Electronic Systems, vol. AES-23, no.1, Jan. 1987, pp. 46-59.

[4] P. Strobach, "New Forms of Least Square Algorithms and Comparison of Their Round Off Error Characteristics," Proc. of the Int. Conf. Acoust., Speech and Signal Processing, Tokyo, Japan, pp. 573-576, 1986.

[5] A. S. El-Fishawy, " Adaptive Algorithms for Change Detection in Image Sequence," Ph.D Dissertation, Drexel University, Philadephia, PA, U.S.A, May 1990.

[6] M. Hadhoud, and D. Thomas, "The Two Dimensional Adaptive LMS (TDLMS) Algorithm," IEEE Trans. Circuits and Systems, vol. 35, no. 5, May 1988, pp. 485-494.

[7] E. H. Satorius and J. Pack, "Application of Least Squares Lattice Algorithms to Adaptive Equalization," IEEE Trans. Communication, vol. COM-29, Feb. 1981, pp. 136-142.

[8] A. Giordano and F. Hsu, "Least Square Estimation with Application to Digital Signal Processing, Prentice Hall,1985

[9] W. Mikhael and F. Yassa," Optimality in the Choice of the Convergence Factor for Adaptive Algorithms, " Proc. IEEE Int. Symp. on Circuits and Systems, Newport Beach, CA, 1983, pp. 1376-1370.

[10] B. Widrow, and S. Stearns, "Adaptive Signal Processing," Prentice-Hall, Englewood Cliffs, N.J., 1985.

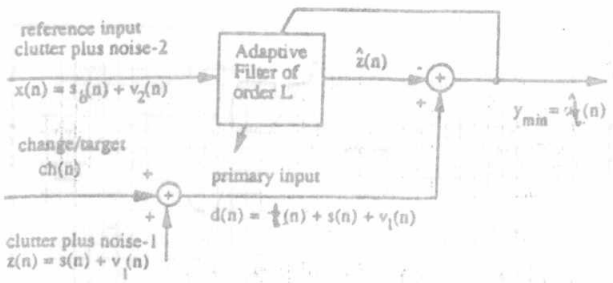

Fig.1 General block diagram of the suggested detectors.

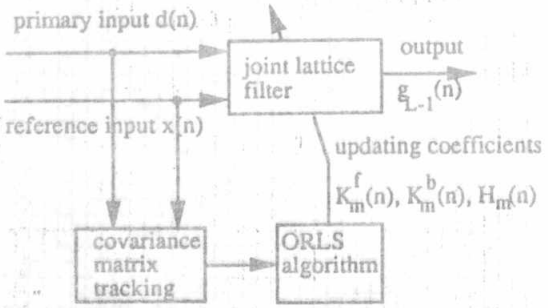

Fig.2 The block diagram of the ORLS lattice algorithm

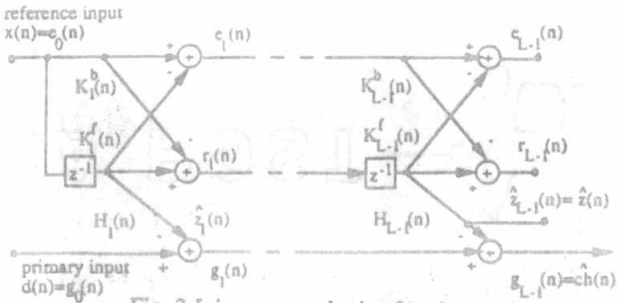

Fig. 3 Joint process lattice for change detection.

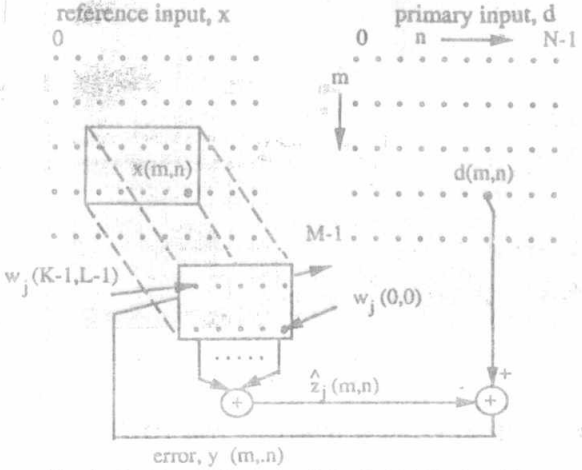

Fig.4 The block diagram of the TDLMS algorithm

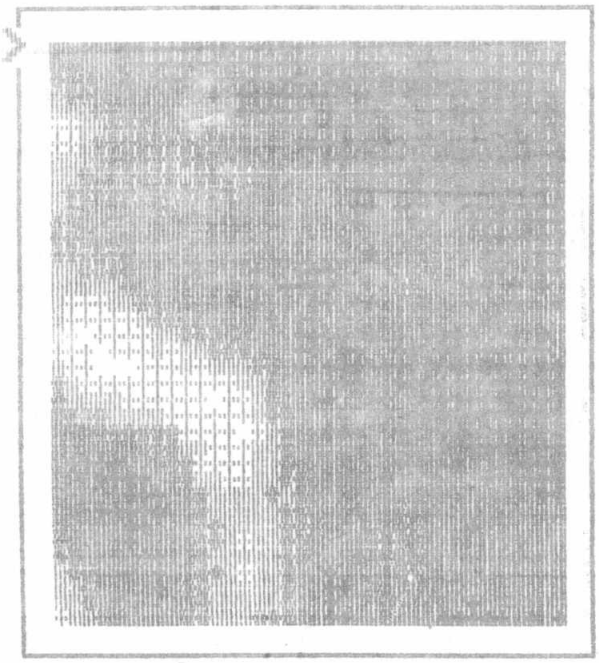

SCNR = -14.49 dB

Fig.6 Primary input image, d(n), with a single pixel target

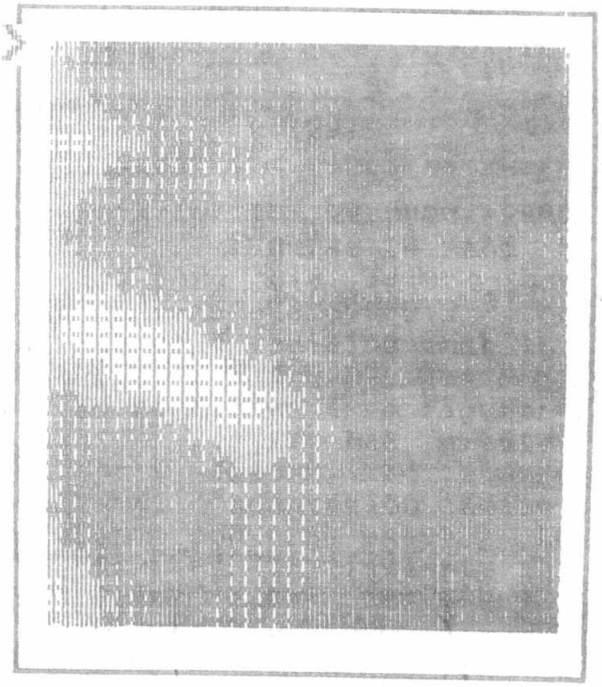

Fig. 7 Reference input image, x(n).

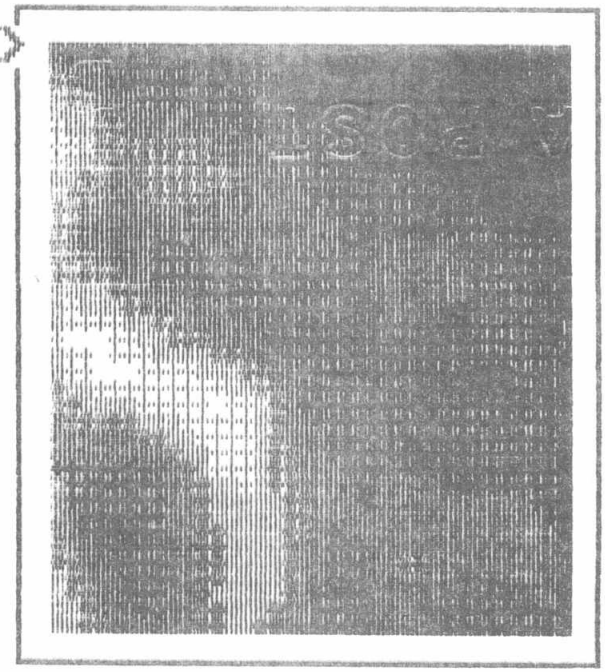

Fig. 5 Optical satellite image, s(n).

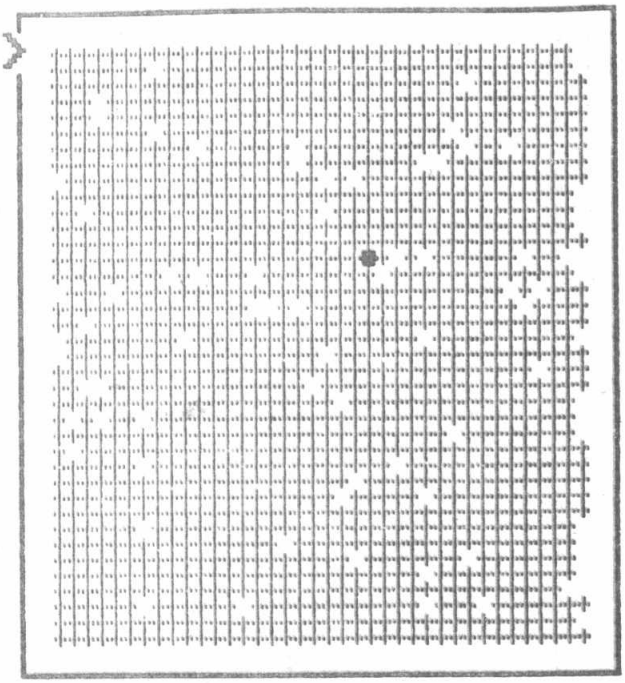

Fig. 8 Output image of the ORLS detector

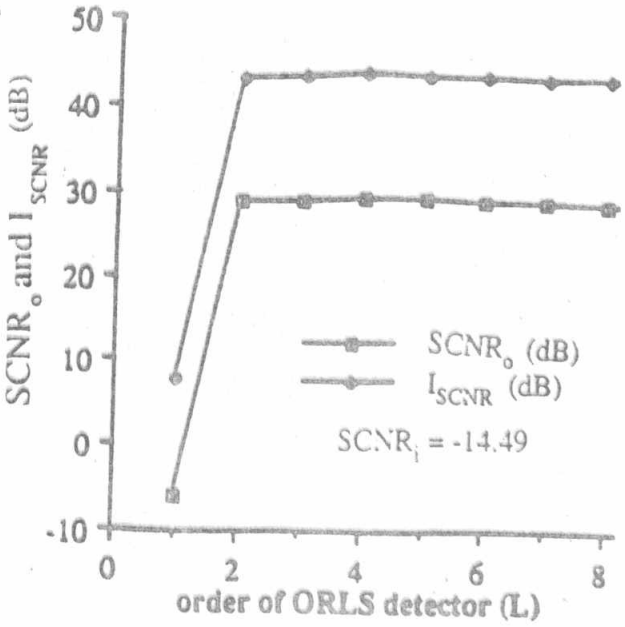

Fig. 6 Effect of the order L of the ORLS lattice on the $SCNR_o$ and the improvement factor.

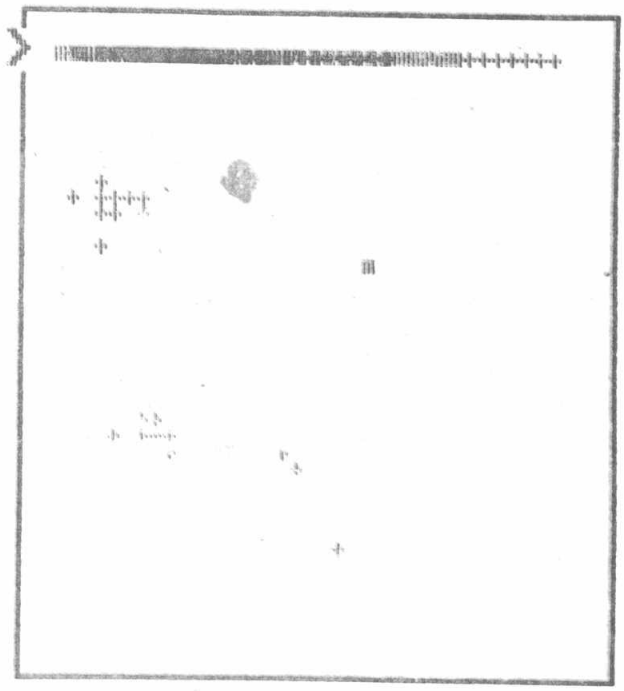

Fig. 9 Output image of the TDLMS detector